

Crystal Chemistry of the Gold (I) Trimer, $\text{Au}_3(\text{NC}_5\text{H}_4)_3$: Formation of Hourglass Figures and Self-Association through Aurophilic Attraction

Akari Hayashi, Marilyn M. Olmstead,* Saeed Attar,† and Alan L. Balch*

Contribution from the Department of Chemistry, University of California,
Davis, California 95616

Received October 24, 2001

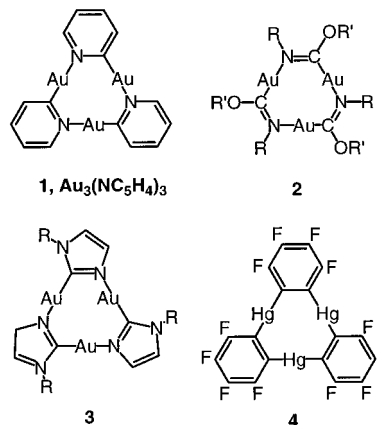
Abstract: X-ray crystallography reveals that individual molecules of $\text{Au}_3(\text{NC}_5\text{H}_4)_3$ self-associate through aurophilic interactions into two distinct structural motifs that involve both extended chains of molecules connected by pairwise $\text{Au}\cdots\text{Au}$ contacts and individual $\text{Au}\cdots\text{Au}$ contacts and discrete dimers linked by pairwise $\text{Au}\cdots\text{Au}$ contacts. The colorless or pale yellow crystals are remarkable for the formation of a distinct hourglass shape within the crystals that develops after months of standing in the atmosphere or after immersion in 4 M hydrochloric acid for a few days. The hourglass figures appear to result from the deposition of gold and are unusual in being formed by a chemical reaction within a crystal rather than as a result of dyeing the crystal during growth.

Introduction

The planar, nine-membered ring complexes shown in Scheme 1, involve three two-coordinate metal ions and have an interesting set of properties that frequently are related to supramolecular aggregation induced by attractive aurophilic interactions. The pyridine-based trimer, $\text{Au}_3(\text{NC}_5\text{H}_4)_3$, **1**, originally prepared by Vaughan over 30 years ago, was the first member of this class of molecules to be synthesized, but its crystal and supramolecular structure have not been reported.¹ Colorless crystals of $\text{Au}_3(\text{MeN}=\text{COMe})_3$, **2**, in which the triangular complexes form prismatic stacks through aurophilic interactions, displays solvoluminescence, solvent-stimulated luminescence from previously photoirradiated crystals.² Fackler and co-workers have shown that complex **3** intercalates Ti^+ or Ag^+ to form crystals containing $\cdots\text{Au}_3\text{Au}_3\text{MAu}_3\text{Au}_3\text{M}\cdots$ ($\text{M} = \text{Ag}^+, \text{Ti}^+$) chains that display luminescence thermochromism.^{3,4} The triangular complexes **2**, **3**, and **4** also form extended structures with organic and inorganic acceptor molecules (*Z*) intercalated between them to form chains with $\cdots\text{Au}_3\text{Au}_3\text{ZAu}_3\text{Au}_3\text{Z}\cdots$ or $\cdots\text{Au}_3\text{ZAu}_3\text{Z}\cdots$ patterns.^{5–7} The

emission spectrum of the crystalline complex formed from **2** ($\text{R} = p\text{-tolyl}$, $\text{R}' = \text{Et}$) and **4** is sensitive to the presence of solvent vapors.⁸

Scheme 1



Attractive interactions between two-coordinate, closed-shell Au(I) ions are important in determining the solid-state structures of many gold (I) complexes. These attractive aurophilic interactions, which have comparable strengths to hydrogen bonds - *ca.* 7–11 kcal/mol, occur when the $\text{Au}\cdots\text{Au}$ separations are less than 3.6 Å.^{9–11} Theoretical studies have shown that this weakly bonding interaction is the result of a combination of correlation effects and relativistic factors.¹²

Here we report on the properties of the pyridine-based trimer, **1**, including both the solid-state supramolecular structure,

* To whom correspondence should be addressed. E-mail: albalch@ucdavis.edu.

† Permanent address: Department of Chemistry, California State University, Fresno, 2555 E. San Ramon Ave., M/S SB70, Fresno, CA 93740-8034.

- (1) Vaughan, L. G. *J. Am. Chem. Soc.* **1970**, *92*, 730.
- (2) Vickery, J. C.; Olmstead, M. M.; Fung, E. Y.; Balch, A. L. *Angew. Chem., Int. Ed. Engl.* **1997**, *36*, 1179.
- (3) Burini, A.; Fackler, J. P., Jr.; Galassi, R.; Peitroni, B. P.; Staples, R. J. *Chem. Commun.* **1998**, 95.
- (4) Burini, A.; Bravi, R.; Fackler, J. P., Jr.; Galassi, R.; Grant, T. A.; Omary, M. A.; Rawashdeh-Omary, M.; Peitroni, B. R.; Staples, R. J. *Inorg. Chem.* **2000**, *39*, 3158.
- (5) Burini, A.; Fackler, J. P., Jr.; Galassi, R.; Peitroni, B. P.; Staples, R. J. *J. Am. Chem. Soc.* **2000**, *122*, 11264.
- (6) Olmstead, M. M.; Jiang, F.; Attar, S.; Balch, A. L. *J. Am. Chem. Soc.* **2001**, *123*, 3260.
- (7) Tsunoda, M.; Gabbai, F. P. *J. Am. Chem. Soc.* **2000**, *122*, 8335.

- (8) Rawashdeh-Omary, M.; Omary, M. A.; Fackler, J. P., Jr. *J. Am. Chem. Soc.* **2001**, *123*, 9689.
- (9) Schmidbaur, H. *Interdiscip. Sci. Rev.* **1992**, *17*, 213.
- (10) Schmidbaur, H. *Chem. Soc. Rev.* **1995**, 391.
- (11) Pathaneni, S. S.; Desiraju, G. R. *J. Chem. Soc., Dalton Trans.* **1993**, 319.
- (12) Pyykkö, P. *Chem. Rev.* **1997**, *97*, 597.

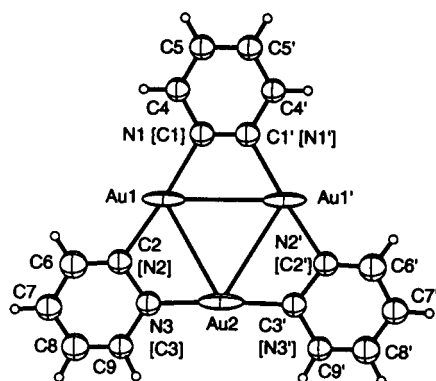


Figure 1. A drawing of molecule 1 of $\text{Au}_3(\text{NC}_5\text{H}_4)_3$ in the crystal. Molecule 2 has a very similar structure with the following replacements: Au3 for Au1, Au4 for Au2 and Au3' for Au1'. For molecule 1, selected bond distances: Au1–N1, 2.07(2); Au1–C2, 2.11(2); Au2–N3, 2.03(3); Au1···Au2, 3.309(2); Au1···Au1', 3.346(3) Å. Selected bond angles; N1–Au1–C2, 174.8(9); N3–Au2–C3', 174.3(13); Au1–N1–C1', 120.2(6); Au1–C2[N2]–N3, 109.8(18); Au2–N3–C2, 124.4(18)°. For molecule 2, selected bond distances: Au3–N10, 2.08(2); Au3–C11, 2.08(2); Au4–N12, 2.06(2); Au3···Au4, 3.3079(19); Au3···Au3', 3.345(3) Å. Selected bond angles: N10–Au3–C11, 178.0(8); N12–Au4–C12', 175.0(11); Au3–N10–C10'', 121.0(5); Au3–C11–N12, 120.5(19); Au4–N12–C11, 117.3(18)°.

formation of novel hourglass figures within the colorless crystals, and the luminescence behavior of the solid.

Results and Discussion

Solid State Structure of $\text{Au}_3(\text{NC}_5\text{H}_4)_3$ 1. Colorless or pale yellow crystals of $\text{Au}_3(\text{NC}_5\text{H}_4)_3$ suitable for X-ray diffraction were obtained by evaporation of a pyridine solution of the complex. There are two, independent half-molecules of the complex in the asymmetric unit. Figure 1 shows a drawing of molecule 1, which is located on a crystallographic mirror plane that lies perpendicular to the molecular plane and passes through Au2. Molecule 2 possesses a similar structure and is similarly situated on a crystallographic mirror plane. Each molecule is planar, but the positions of the coordinating carbon and nitrogen atoms are disordered with site occupancies of 0.5. The Au···Au distances within the two molecules fall in the range 3.3079–(19)–3.346(3) Å, which is similar to the range of distances (3.274–3.339 Å) found in a number of solids containing the related triangular complex, $\text{Au}_3(\text{MeN}=\text{COMe})_3$.²

Individual molecules of $\text{Au}_3(\text{NC}_5\text{H}_4)_3$ self-associate through aurophilic interactions into two distinct motifs as shown in Figure 2. Figure 3 presents a stereoscopic view of the unit cell that shows how the two structural motifs are arranged, while Figure 4 shows a projection down *c* which emphasizes the organization of the dimers and the extended chains into layers. Molecule 1 forms an extended chain as seen in part A of Figure 2. Within this chain the triangular complexes form two types of Au···Au contacts between adjacent molecules. Thus, there are pairwise contacts that involve interactions between Au1 and Au1a along with an equivalent interaction between Au1c and Au1b. The intermolecular Au1···Au1a distance is 3.146(3) Å. Additionally, there is a single Au2···Au2d interaction at the other end of the molecular triangle with a distance of 3.077(2) Å. In the extended chains formed by molecule 1, each individual gold ion makes contact with one other gold ion. In contrast, in the extended prismatic stacks in $\text{Au}_3(\text{MeN}=\text{COMe})_3$ ¹ each gold ion makes contact with two neighboring gold ions. Unlike

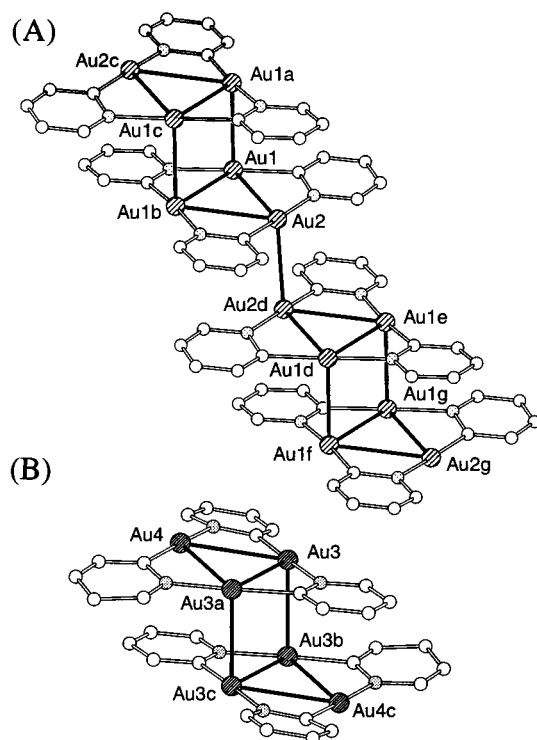


Figure 2. Drawings which show the self-association of (A) molecule 1 into extended chains through two types of Au···Au interactions and (B) molecule 2 into a dimer. Distances: Au1···Au1a, 3.146(3); Au2···Au2d, 3.146(3); Au3···Au3b, 3.105(2) Å.

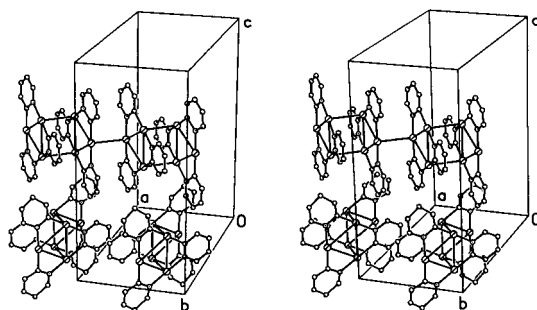


Figure 3. A stereoscopic view of the unit cell of $\text{Au}_3(\text{NC}_5\text{H}_4)_3$.

molecule 1, molecule 2 forms a simple dimer with a set of two intermolecular Au···Au contacts. These contacts are shown in part B of Figure 2 and involve pairwise interactions between four Au3 ions. The Au3···Au3b distance is 3.105(2) Å. Notice that all the intermolecular Au···Au contacts in this solid are shorter than the intramolecular Au···Au contacts. The next nearest Au···Au contact, which involves Au4, is 4.965 Å. The formation of a dimer through pairwise interactions as seen in part B of Figure 2 has been observed previously in the structure of $\text{Au}_3(\text{MeC}_6\text{H}_4\text{N}=\text{COMe})_3$ and other complexes.^{4,7,13} However, the formation of extended chains that involve this dimer motif coupled with a single Au···Au contact at the opposite end of the molecule is unprecedented for a planar gold (I) complex of the types shown in Scheme 1. Likewise, the presence of two different types of intermolecular aurophilic interactions in one crystal is unusual. However, in the solid state $\{[(\text{Me}_3\text{P})\text{Au}]_3\text{S}\}^+$ does display a chain motif that includes alternating single and double sets of Au···Au contacts.¹⁴

(13) Tiripicchoi, A.; Tiripicchio Camellini, M.; Minghetti, G. *J. Organomet. Chem.* **1979**, *171*, 399.

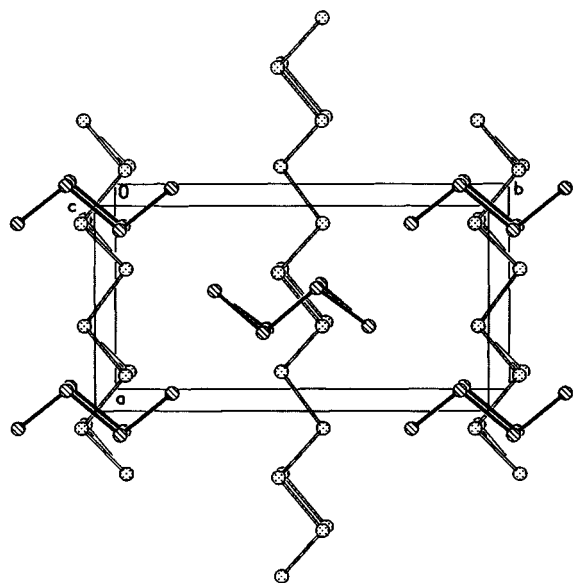


Figure 4. A view of the unit cell of $Au_3(NC_5H_4)_3$ projected down the c axis. Only the locations of the gold ions are shown.

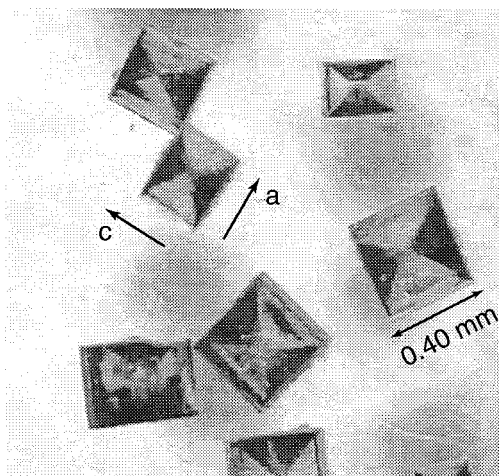


Figure 5. A photomicrograph of crystals of $Au_3(NC_5H_4)_3$ after several months of atmospheric exposure. The directions of the crystallographic a and c axes are shown beside one of the crystals, while a dimension of one of the crystals is also shown.

Formation of Hourglass Figures in Crystals of $Au_3(NC_5H_4)_3$, 1. For an organometallic complex, crystals of $Au_3(NC_5H_4)_3$ are particularly stable and retain their crystallinity after weeks of atmospheric exposure. However, some light fogging of the crystal surfaces becomes apparent after several days in the atmosphere.

More interestingly, however, is the gradual appearance of a distinct hourglass shape within the crystals that develops after months of standing in the atmosphere. Figure 5 shows a photograph of crystals of $Au_3(NC_5H_4)_3$ at this stage. Visual observation of the crystals under an optical microscope reveals that the hourglass shape has a distinct golden color, and it appears that metallic gold is deposited within the crystals in specific regions. However, the X-ray diffraction from crystals with the hourglass shapes clearly developed does not display any detectable changes. No additional features that could be ascribed to metallic gold could be seen because of either the

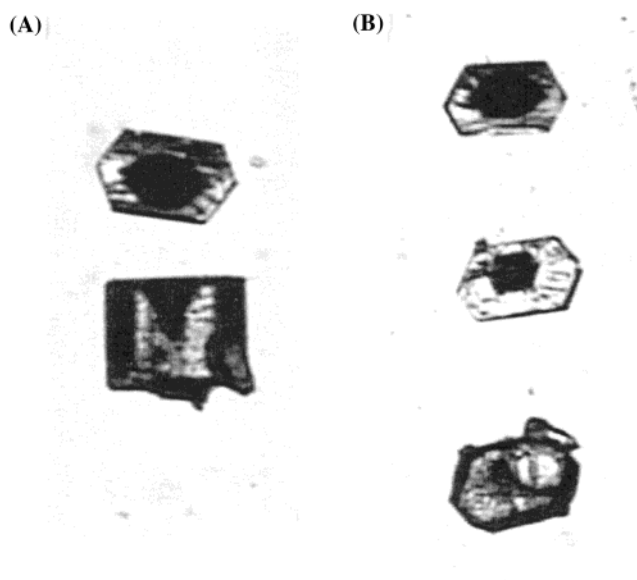


Figure 6. (a) Photomicrograph of (bottom) a crystal of $Au_3(NC_5H_4)_3$ after several months of atmospheric exposure and (top) a slice taken from that crystal and turned on its side so that the c axis is perpendicular to the plane of the image. (b) Photomicrograph of successive slices cut from that crystal.

small amount of material in the hourglass figures, the small size of the particles, or its lack of crystallinity. Using polarized light the hourglass inclusion region of the crystal shows up as a distinct domain. A data set was collected on a crystal with this domain excised, but there was no significant change in the structure.

All crystals (whether fresh or darkened) can easily be cut into slices perpendicular to c . Figure 6A shows a piece cut from the larger crystal as it appears when turned onto its side. Notice that the darkened patch does not reach entirely to the edges of the slice. Figure 6B shows a succession of slices, indicating that the darkened patch reaches into the crystal in diminishing size. This evident cleavage plane can be traced to the crystal structure because there are no strong intermolecular interactions between species in this plane. From Figure 3 it can be seen that only nonoverlapping rows of pyridine rings are arranged in the structure in this direction. To further clarify the arrangement of species in the structure, Figure 4 focuses on the arrangement of alternating layers of Au dimers and polymers along the c direction. Keeping in mind that the bridging pyridines are coplanar with Au triangles, it is apparent that the edges of the Au triangles as well as these connecting pyridines are all vertical in the drawing. As viewed down the c axis (Figure 4), there is a superposition with a 90° rotation of Au dimers on top of Au polymers. The morphology of the exposed surface of interest will likely consist of edges of pyridines, which, if lost forming either pyridine or bipyridine, will ultimately become a layer of gold. If such a layer shifts with respect to the layer below, a cause for the stacking fault can be found.

These hourglass figures resemble the patterns of dye inclusions in otherwise transparent crystals that are obtained by growing certain crystals in the presence of chromophoric or luminophoric molecules.¹⁵ However, the patterns seen in Figure 1 develop in the crystals after crystal growth is complete and,

(14) Angermaier, K.; Schmidbaur, H. *Chem. Ber.* **1994**, *127*, 2387.

(15) Kahr, B.; Gurney, R. W. *Chem. Rev.* **2001**, *101*, 893.

as shown below, result from a chemical reaction occurring within the crystals.

Crystals of **1** invariably form with a stacking defect that is pronounced along the crystallographic *c* axis. As shown in Figure 1, only the gold ions were assigned anisotropic thermal ellipsoids, and these are highly anisotropic. In Figure 1, the thermal ellipsoids are depicted at the 50% probability level. The ratio of the maximum to minimum values of the diagonal tensor values, U_{33}/U_{11} , are 15.2, 13.2, 29.5, and 60.8 for Au1, Au2, Au3, and Au4, respectively. These prolate ellipsoids are all pointed in the direction of the *c* axis, which is also the direction of the hourglass inclusions. All crystals examined (four complete data sets) have this defect. If there is a correspondence between these defects, the dark patterns that develop, and the crystal packing arrangement, it is not readily apparent from inspection of Figure 3. Doping of an impurity, such as pyridine, is a likely cause of the stacking defect, but its presence has not, as yet, been detected.

Likely factors involved with the formation of these hourglass figures have been examined. Since many gold (I) complexes are photosensitive, we initially believed that the figures were produced by exposure to room light. However, exposure to a lamp for 1 day led only to a uniform blackening of the crystal surface without the formation of the hourglass figures seen in Figures 5 and 6. Formation of these figures is, however, hastened when the crystals are immersed in water. Crystals stored at room temperature in the dark under a dinitrogen atmosphere showed no changes after 15 weeks. Those immersed in water with a pH of 6 in the dark develop visible hourglass figures after 9 weeks. Immersion in water with a pH of 2 produced the hourglass figures after 5 weeks. Placing a crystal in 4 M hydrochloric acid produces the hourglass figures within a few days. Consequently, hydrolysis of $\text{Au}_3(\text{NC}_5\text{H}_4)_3$ may initiate the formation of the hourglass patterns. It is known that $\text{Au}_3(\text{NC}_5\text{H}_4)_3$ undergoes thermal decomposition to yield metallic gold and bipyridine,¹ and a similar reaction to form gold and bipyridine but triggered by the presence of acid may be responsible for the formation of these hourglass figures. Thus, it appears that specific regions within crystals can promote chemical reactions.

Luminescence of $\text{Au}_3(\text{NC}_5\text{H}_4)_3$, **1.** In pyridine solution $\text{Au}_3(\text{NC}_5\text{H}_4)_3$ is colorless with an absorption maximum at 340 nm. Solutions of $\text{Au}_3(\text{NC}_5\text{H}_4)_3$ are faintly luminescent with $\lambda_{\text{max}} = 425$ nm. The crystals are also colorless or pale yellow but luminescent when initially prepared. Figure 7 shows the emission ($\lambda_{\text{max}} = 490$ nm) and excitation spectra of the solid. Since the onset of the excitation spectrum appears well before the absorption maximum observed in solution and the luminescence differs in the solid state and solution, the luminescence properties of the solid are not simply those of the molecular entity (as found in solution). Rather they are the result of the extended supramolecular aggregation seen in the solid in Figure 3. Thus, they are related to the emission properties of $\text{Au}_3(\text{MeN}=\text{COMe})_3$, **2**, in that the supramolecular aggregation influences the luminescence. However, $\text{Au}_3(\text{NC}_5\text{H}_4)_3$ is not solvoluminescent, nor does it display the very long-lived emission observed for $\text{Au}_3(\text{MeN}=\text{COMe})_3$, **2**.² Crystals of $\text{Au}_3(\text{NC}_5\text{H}_4)_3$, **1**, do not emit light when they are subject to the mechanical stress of grinding, and thus there is no evidence

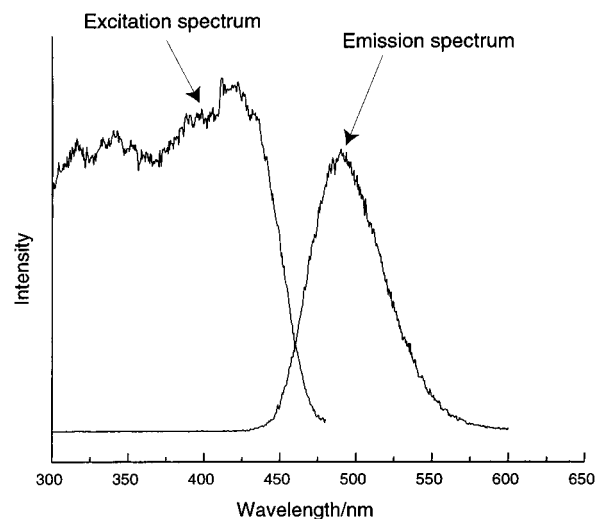


Figure 7. Excitation ($\lambda_{\text{em}} = 490$ nm) and emission ($\lambda_{\text{exc}} = 290$ nm) spectra of $\text{Au}_3(\text{NC}_5\text{H}_4)_3$ in the solid state.

that the crystals display triboluminescence.¹⁶ Crystals which have developed the hourglass figures remain luminescent.

Experimental Section

Preparation of Compounds. $\text{Au}_3(\text{NC}_5\text{H}_4)_3$ was prepared as described previously¹ and recrystallized from hot pyridine.

X-ray Data Collection. Crystals were coated with a light hydrocarbon oil and mounted on a glass fiber in the cold dinitrogen stream of the diffractometer. Data were collected on a Siemens R3m/V diffractometer with graphite monochromated Mo K α radiation. Lorentz and polarization corrections were applied. A 1.7% decay in the intensities of two check reflections monitored every 200 reflections was observed. The intensity data were scaled using a linear correction for the observed decay. An empirical absorption correction utilizing equivalents was employed.¹⁷ Crystal data for $\text{Au}_3(\text{NC}_5\text{H}_4)_3$ pale-yellow block, formula $\text{C}_{15}\text{H}_{12}\text{Au}_3\text{N}_3$, fw 825.18, crystal dimensions 0.22 mm \times 0.16 mm \times 0.14 mm, orthorhombic, space group *Pbam*, $a = 9.184(2)$ Å, $b = 17.409(4)$ Å, $c = 18.815(4)$ Å, $V = 3008.2(11)$ Å³, $\lambda = 0.71073$ Å, $Z = 8$, $D_c = 3.644$ Mg m⁻³; $\mu(\text{Mo K}\alpha) = 29.18$ mm⁻¹; ω scans, $2\theta_{\text{max}} = 45^\circ$; $T = 140(2)$ K; 6474 reflections collected; 1998 independent ($R_{\text{int}} = 0.064$) included in the refinement; min/max transmission = 0.060/0.106.

Solution and Structure Refinement. Calculations for the structures were performed using SHELXS-97 and SHELXL-97. Tables of neutral atom scattering factors, f' and f'' , and absorption coefficients are from a standard source.¹⁸ The structure was solved by a combination of Patterson and difference Fourier methods and refined by full-matrix least-squares based on F^2 ; $R1 = 0.113$, $wR = 0.155$ for all data; conventional $R1 = 0.052$ computed for 1142 observed data ($>2 \sigma(I)$) with no restraints and 99 parameters. Only the gold atoms were refined anisotropically. All hydrogen atoms were placed geometrically and included through the use of a riding model.

The structure can also be solved and refined in the monoclinic system, space group *P2₁/c*, with $a = 18.815(4)$ Å, $b = 9.184(2)$ Å, $c = 17.409(4)$ Å, $\beta = 90.06(3)^\circ$. Apart from minor variations in individual bonds, the structure is identical. The problem areas are not eliminated in this space group. Reduction in the symmetry of the cluster does not remove the disorder seen in the interchange of the coordinated C and N atoms, and the anisotropic thermal ellipsoids for the gold atoms are still elongated in the direction of the longest axis (the *a* axis in this

(16) Zink, J. I. *Acc. Chem. Res.* **1978**, *11*, 289.

(17) ψ -scans (G. M. Sheldrick) based on a method of R. H. Blessing, *Acta Crystallogr., Sect. A* **1995**, *A51*, 33.

(18) *International Tables for Crystallography*; Wilson, A. J. C., Ed.; Kluwer Academic Publishers: Dordrecht, 1992; Volume C.

setting). The final R1 value of 0.058 is only slightly larger than in the orthorhombic case. We have chosen to present the structure in the higher-symmetry space group (orthorhombic, *Pbam*) as this is most often the correct choice.

Acknowledgment. We thank the National Science Foundation (CHE 9610507 and 0070291 to A.L.B.) and the Petroleum Research Fund for support.

Supporting Information Available: X-ray crystallographic data collection and structure refinement, tables and atomic coordinates, bond distances and angles, anisotropic thermal parameters, and hydrogen atom positions for $Au_3(NC_5H_4)_3$ in CIF format. This information is available free of charge via the Internet at <http://pubs.acs.org>.

JA012416Y